Intravenous Immunoglobulin with Enhanced Polyspecificity Improves Survival in Experimental Sepsis and Aseptic Systemic Inflammatory Response Syndromes

Running Head: Modified IVIg improve survival in sepsis

Iglika Djoumerska-Alexieva[1], Lubka Roumenina[2], Anastas Pashov[1], Jordan Dimitrov[1,2], Maya Hadzhieva[1], Sandro Lindig[3], Elisaveta Voynova[4], Petya Dimitrova[1], Nina Ivanovska[1], Clemens Bockmeyer[7], Zvetanka Stefanova[1], Catherine Fitting[5], Markus Bläss[3], Ralf Claus[3], Stephan von Gunten[6], Srini Kaveri[2], Jean-Marc Cavaillon[5], Michael Bauer[3] and Tchavdar Vassilev[1,3*]

Keywords: antibody polyspecificity, IVIg, passive immunotherapy, sepsis, systemic inflammation

[1] Department of Immunology, Stefan Angelov Institute of Microbiology, Bulgarian Academy of Sciences, 1113 Sofia, Bulgaria
[2]INSERM UMRS 1138, Centre de Recherche des Cordeliers, 75006 Paris, France
[3]Center for Sepsis Control and Care, University Hospital, Friedrich Schiller University, 07747 Jena, Germany
[4]Laboratory of Immunogenetics, National Institute of Allergy and Infectious Diseases, National Institutes of Health, Rockville MD, USA
[5]Cytokines & Inflammation Unit, Institut Pasteur, 75724 Paris, France
[6]Institute of Pharmacology, University of Bern, 3010 Bern, Switzerland
[7]Institute of Pathology, Hannover Medical School, Hannover, Germany

*Correspondence to:
Tchavdar Vassilev, M.D., Ph.D.
Department of Immunology,
Steffan Angelov Institute of Microbiology
Bulgarian Academy of Sciences
26, Acad. Georgi Bonchev St., 1113 Sofia, Bulgaria
Tel.: +359-2-979 6348; Fax: +359-2-870 0109
e-mail: vassilev@microbio.bas.bg and tchavdarv@gmail.com

Abstract

Sepsis is a major cause for death worldwide. Numerous interventional trials with agents neutralizing single pro-inflammatory mediators have failed to improve survival in sepsis and aseptic systemic inflammatory response syndromes. This failure could well be explained by the widespread gene expression dysregulation known as “genomic storm” in these patients. A multifunctional polyspecific therapeutic agent might be needed to thwart the effects of this "storm". Licensed pooled intravenous immunoglobulin preparations seemed to be a promising candidate but they have also failed in their present form to prevent sepsis-related death. We report here the protective effect of a single dose of intravenous immunoglobulin preparations with additionally enhanced polyspecificity in three models of sepsis and aseptic systemic inflammation. The modification of the pooled immunoglobulin G molecules by exposure to ferrous ions resulted in their newly acquired ability to bind some pro-inflammatory molecules, complement components and endogenous “danger” signals. The improved survival in endotoxemia was associated with serum levels of pro-inflammatory cytokines, diminished complement consumption and normalization of the coagulation time. We suggest that intravenous immunoglobulin preparations with additionally enhanced polyspecificity have a clinical potential in sepsis and related systemic inflammatory syndromes.

Introduction

Sepsis remains a leading cause of death in intensive care units. It is the result of a severe and uncontrolled activation of inflammatory and coagulation pathways in response to infection, accompanied by a variable degree of immune paralysis (1-3). Despite adequate antibiotic therapy and the use of sophisticated life-supporting measures the prognosis of patients with this syndrome has only marginally improved in recent years. This frustrating lack of progress, especially when novel experimental treatments aimed to target individual mediators of inflammation were used, has been hard to explain so far (1, 2, 4, 5).

A recent study has found significant changes of expression patterns of more than 80% of human genes (referred to as "genomic storm") in trauma patients and bacterial LPS-injected volunteers with severe inflammatory response syndrome (SIRS) (6). This "genomic storm" could well explain the discouraging results from the efforts to treat severe generalized inflammatory syndromes by neutralizing a single pro-inflammatory mediator. Targeting only one or very few components in a system-wide network disturbance, may not be successful in exerting control. A multifunctional therapeutic agent may be needed instead. Passive immunotherapy with pooled immunoglobulin preparations (administered as intravenous immunoglobulin, IVIg) is a logical choice as they contain a vast array of antibody specificities, some of which could well affect key products of the genomic storm. In addition to antibodies that neutralize pathogens and their virulence factors, IVIg have diverse immunomodulatory and anti-inflammatory activities (7). The latter are mediated through versatile interactions with receptors on immune cells, components of the complement system, cytokines, etc. The outcome is down-regulation of T-, B-lymphocyte activity and dendritic cell functions and modulation of the cytokine network (for

review see (7, 8)). The results from numerous clinical trials, using IVIg infusions as adjunctive therapy in sepsis patients have been, however, inconclusive (3, 9-11).

All commercially available IVIg preparations are generally believed to have identical biological and therapeutic properties. This may not be the case as the licensed therapeutic immunoglobulins, produced using a fractionation step at pH 4.0 have been shown to possess an increased potential to bind to self-antigens (12). Importantly, this increased reactivity to antigens correlates with different functional activity of immunoglobulin preparation (13, 14). Thus, the administration of the acid pH-treated, but not of the same unmodified preparation significantly decreased mortality in animals with endotoxemia (12, 13). Previous studies by our and other groups have proven that, in addition to low pH buffers, the exposure to a number of other substances (e.g. ferrous ions, heme, reactive oxygen species, etc.) also increases the antigen-binding polyspecificity of some IgG molecules (5, 15-17). IVIg modified by Fe(II) exposure acquired the ability to bind to the human pro-inflammatory cytokine IFN-γ and to improve survival in mice injected intravenously with 5.10^8 live *E. coli* or i.p with bacterial LPS (15, 18). Infusions of Fe-ions modified IVIg were also shown to have an anti-inflammatory activity in an experimental diabetes model (14). On the basis of these preliminary data we have hypothesized that the passive immunotherapy with pooled immunoglobulin preparations with additionally enhanced polyspecificity could neutralize some of the products of the genomic storm and thus should be beneficial in systemic inflammatory syndromes regardless of their primary insult. Three models of systemic inflammation in the presence or absence of infection were used to check this hypothesis: induced by LPS, by zymosan and by cecal ligation and puncture (CLP). While the infusion of native IVIg had no effect on survival, the administration of the same single dose of the Fe(II)-exposed IVIg improved significantly the survival of mice in all three models.

The studies of the mechanisms of beneficial action of the latter preparation revealed its ability to bind to pro-inflammatory molecules, complement components and extracellular histones.

Materials and Methods

Mice

Outbred female ICR mice (8-12 weeks old, 18-22 g) were purchased from the Breeding Farm of the Bulgarian Academy of Sciences and kept in a conventional animal facility. C57Bl/6 mice (8-12 weeks old, 18-22 g) were from Charles River Laboratories, Sulzfeld, Germany. The animals were housed under specific pathogen-free conditions, 6 per cage, with *ad libitum* access to food and water and maintained in a temperature-controlled environment. The animals were allowed to adapt to laboratory conditions for three days. The experimental protocols were approved by the Animal Care Commission of the Institute of Microbiology and the Thuringian State Office for Consumer Protection and Food Safety in accordance with National and European Regulations.

Blood (0.05 ml / mouse) was collected from the retro-orbital sinus by a Pasteur pipette after a local anesthesia with 0.5% tetracaine hydrochloride and let to clot at +4 ^{0}C. Sera samples were aliquoted and stored at -80 $^{\circ}$C.

Experimental sepsis models

All survival experiments were performed using ICR mice in groups of twelve animals each. Endotoxemia was induced by the i.p. injection of 10 mg/kg *E. coli* LPS (B 055:B5, #L2880, Sigma-Aldrich St. Luis, MO). Cecal ligation and puncture (CLP) was performed as described in the literature (19). Briefly, the mice were anesthetized i.p. with ketamine (80 mg/kg) and xylazine (10 mg/kg), a 1.5 cm long laparotomic incision was made, the cecum was ligated at 2/3

of its length and punctured once by a sterile 21*G* needle. The puncture was confirmed by a delicate pressing and the abdomen was closed by suture. No antibiotics or fluids were administered. Multiple organ dysfunction was induced by the intraperitoneal injection of 500 mg/kg zymosan (Sigma-Aldrich) (20). The dose of the LPS or zymosan was adjusted to cause 80 to 100% mortality in the control animals, treated with PBS only.

Modified pooled therapeutic human immunoglobulins

The intravenous immunoglobulin preparations Endobulin S/D (Baxter, Deerfield, IL) and a special maltose- and albumin-free batch of Immunovenin-intact (BulBio Ltd, Sofia, Bulgaria, kindly provided by Dr Julia Nacheva), were used in the experiments. Both preparations are referred to as “native”, as they are produced without using a fractionation step at acid pH (12). The pooled immunoglobulins were exposed to freshly prepared ferrous sulfate solution (1 mM final concentration) for 2 h at 4°C and then dialyzed against phosphate-buffered saline (PBS; pH 7.4) for at least 48 h as previously described (15). In a separate experiment the ferrous ions-modified IVIg was dialyzed against 4 mM EDTA in PBS and then against PBS.

Treatment schedules

Single dose of the native, the modified IVIg preparations or PBS alone was injected intravenously (i.v.) 10 min before the administration of LPS, of zymosan or at the beginning of CLP procedure. In all experiments survival was observed daily for seven days.

In a separate experiment groups of animals were treated i.v. with 50 mg/kg of the native or Fe(II)-exposed IVIg at different time points – minutes before, one, or four hours post-LPS injection.

Determination of serum levels of cytokines

The levels of TNF-α, IFN-γ, IL-6, IL-10 and IL-22 in the sera obtained 4, 24 and 48 h after LPS injection were measured using commercial ELISA kits (PeproTech EC Ltd., London, UK).

The Mouse inflammation antibody array kit (RayBiotech Inc., Norcross, GA). was used to evaluate semi-quantitatively the levels of 40-inflammation-related molecules. Briefly, membranes spotted with 40 capture antibodies were blocked with the manufacturer's BSA buffer and incubated with the studied serum samples for 2 h at room temperature. After washing, a cocktail of biotinylated anti-cytokine antibodies was incubated with membranes for 2 h at room temperature. Membranes were then washed, incubated with HRP-conjugated streptavidin for 2 h, washed and exposed to the ECL peroxidase substrate for 2 minutes. Next, the membranes were drained and exposed for 20 seconds to a X-ray film (Kodak X-Omat AR film). The gray color intensity of the spots was quantified by densitometry and analyzed using the Image-Tool v2.0 for Windows (UTHSCSA, San Antonio, TX, USA) software package.

Measurement of plasma C3 levels

The C3 levels in plasma were measured at 4, 24 and 48 hour after LPS administration using the Mouse C3 ELISA kit (GenWay Biotech Inc., San Diego, CA).

Binding of modified IVIg to the C1q complement component and biological activity assays

Increasing concentrations of native and of ferrous ions exposure-modified IVIg were added to the wells of a plate coated with human C1q (Calbiochem, Merck KGaA, Darmstadt, Germany).

Bound IgG was detected using anti-human IgG-HRP, (Fc-specific, from Southern Biotech) and OPD substrate.

The ability of modified IVIg to interfere with the binding of human C1q to its ligands was analyzed by ELISA. C-reactive protein (from Calbiochem) or human IgG_1 were coated to the plates at a concentration of 10 µg/ml and the wells were blocked with 2% BSA. IVIg (at 10 mg/ml) was pre-exposed to ferrous ions (0; 0,5 and 1mM) and was mixed at 1,5 mg/ml in the wells of a second plate with increasing concentrations of C1q (7 serial dilutions starting from 10µg/ml). The mixtures were transferred to the CRP- and human IgG_1-coated plates. After incubation for 1 h at 37 ^{o}C and extensive washing, anti-C1q biotin-conjugated antibody (purified from goat anti-C1q antiserum from Quidel, San Diego, CA and biotinilated in house) was added in a 1:500 dilution. Finally streptavidin-HRP was added (from DAKO, diluted 1:1000) for 30 minutes. After washing TMB substrate was used, the reaction was stopped with 2M sulfuric acid and the optical density was read at 450 nm.

Coagulation and organ dysfunction tests

Coagulation time was measured as previously described (21). Animals were bled 4 hours after the injection of LPS and the plasma concentrations of bilirubin and creatinine were measured by commercially available kits (from DIALAB GmbH, Wr. Neudorf, Austria).

Detection of antibodies to cytokines and endogenous «danger» molecules in the immunoglobulin preparations

The Bio-Plex Cytokine Assay (BioRad, Richmond, CA) was used to detect antibodies to human IL-1Ra, IL-6, IL-8, IL-10, IL-15, TNF, G-CSF, IFN-γ, IP-10, RANTES, MCP-1, MIP-1 alpha

and MIP-1 beta in a) the native IVIg, b) Fe(II) –exposed IVIg and c) pooled human IgM (kindly provided by Biotest AG, Dreieich, Germany). A human IgG1 monoclonal antibody was used as a control (22). The immunoglobulin preparations were added (at a concentration 200 µg/ml) to serial dilutions of the respective cytokines and incubated for 1 h at 37 °C following the manufacturer's protocol. The presence of antibodies to mouse IFN-γ, human MIG, HMGB1 (from HMGBiotech, Milan, Italy), recombinant human heat shock proteins (HSP 60 and HSP 70 obtained from Enzo Life Sciences, Lausen, Switzerland) and to human histones H3 and H4 (Roche Diagnostics, Mannheim, Germany) were tested for by ELISA. Plates (Nunc MaxiSorp) were coated with 2 µg/ml of the respective antigens in 0.1 M carbonate buffer and incubated overnight at 4 °C. After blocking and washing, the plates were incubated for 2 h at room temperature with increasing concentrations of the immunoglobulin preparations under study. The plates were then extensively washed and goat anti-human IgG antibody coupled to alkaline phosphatase was added and incubated for 1 h at room temperature. Immunoreactivities were revealed with p-nitrophenyl phosphate (Sigma-Aldrich) and the OD values were read at OD=405 nm.

Statistical analysis

All statistical analyses were performed using the GraphPad Prism 4 software (La Jolla, CA, USA) and the R software (v.3.0.2). Data were expressed as mean ± SD. Differences in survival curves were compared using the Mantel-Haenszel test. For other data, the differences in the mean values between groups were analyzed with the two-tailed Student *t* test. Differences were considered significant when $p < 0.05$. Pearson correlation coefficient was used to compare gene expression profiles in different organs.

Results

Protective effect of ferrous ions-exposed IVIg improved survival in sepsis and aseptic SIRS

The intravenous administration of a single dose of 50 mg/kg of the Fe(II)-ions-modified IVIg significantly decreased the mortality of animals with endotoxemia (Fig. 1A - left panel). The same treatment (at dose of 250 mg/kg) was protective in zymosan-induced SIRS and in polymicrobial CLP sepsis (Fig. 1A, middle and right panels). The survival curves of all animals in the experimental series are shown on Fig. S1. The native immunoglobulin preparation, regardless of the dose used, had no effect thus confirming results from numerous clinical trials.

The mechanisms of protective activity of IVIg with enhanced polyspecificity in endotoxemia were studied in more details. The infusion of the modified IVIg one hour post-LPS injection still had a protective effect while the treatment delayed for 4 hours failed to improve the survival (Fig. 1B). The iron content of IVIg increased after the Fe(II) treatment from 0.028 mg/g IgG to 7.2 mg/g IgG (Table S1). Nevertheless the beneficial effect of the preparation was still present even upon dialysis against EDTA which decreased the iron concentration (Fig. 1C).

Gene expression analysis

Microarray data of organ samples from Fe(II)-exposed IVIg treated endotoxemic mice were clustured by an unfiltered unsupervised approach. Unique responses to Fe(II)-exposed IVIg were observed in all organs, but were most pronounced in the liver, supported by a weaker correlation (Pearson correlation coefficient r (IVIg vs Fe(II)-exposed IVIg) = 0.83 in kidney and r = 0.45 in liver). Although, several differentially expressed genes (DEG) could be identified, they did not constitute an easily interpretable pattern of signaling pathways (Figure S2).

Treatment with IVIg with enhanced polyspecificity affects plasma levels of pro- and anti-inflammatory cytokines

IVIg exposure to Fe(II) ions did not result in its enhanced binding to bacterial LPS (Fig. S3), indicating that the beneficial effect of modified IVIg was due to its interactions with host defense mechanisms rather than to a direct neutralization of LPS. The observed beneficial effect on survival suggests that the levels of pro-inflammatory molecules might be influenced by the treatment. Indeed, plasma levels of TNF-α, IL-6 and IFN-γ were significantly reduced in animals injected with modified IVIg (Fig. 2A). In contrast, the levels of IL-10 and IL-22 were significantly elevated. A semi-quantitative dot-blot protein array technique allowed the analysis of a larger panel of inflammation-related molecules. Significantly lower levels of IL-6, LIX (CXCL5), IL-12p70 and MIP-1gamma (CCL9) were detected after treatment with the IVIg with increased polyspecificity (Fig. 2B, 2C).

Effect of ferrous ions-exposed IVIg on the complement system, coagulation and organ dysfunction of mice with LPS-induced sepsis

Complement activation and the release of anaphylatoxins play an important role in the pathogenesis of sepsis (23, 24). The levels of C3 complement component in the circulation mirror the severity of on-going inflammation. The LPS injection resulted in a sharp and prolonged drop in C3 levels and the administration of the native IVIg did not significantly affect this level. Interestingly, the infusion of the same single dose of the IVIg with enhanced polyspecificity led to a significantly diminished consumption of C3 (Fig. 3A). We analyzed in more detail the interaction of the immunoglobulin preparations with human complement components. The binding of the pooled human IgG to the C1q component was enhanced after its

exposure to ferrous ions (Fig. 3B). While the pre-incubation of C1q with Fe(II)-exposed IVIg did not affect the interaction of the latter with immobilized IgG1 (not shown), it significantly inhibited C1q binding to CRP (Fig. 3C). Interestingly, the modified immunoglobulin preparation bound to C3a, but not to C5a anaphylatoxins (Fig. 3D).

Systemic inflammation in sepsis is accompanied by an over-activation of the coagulation cascade and results in disseminated clots in small blood vessels, contributing to organ failure. A single infusion of ferrous ions-exposed IVIg to endotoxemic mice normalized the blood clotting time (Fig. 3E). This could well explain also the observation that liver injury was significantly ameliorated in the group treated with the modified IVIg as assessed by the capacity of ferrous ions-exposed IVIg to decrease the LPS-induced elevation of serum bilirubin levels (Fig. 3F). Creatinine levels at the same early time point were not affected.

The Fe(II)-modified IVIg acquires additional polyspecificity that includes ability to bind pro-inflammatory mediators and endogenous “danger” molecules

The exposure of therapeutic IVIg to increasing concentrations of ferrous ions results in its ability to bind to a broader number of antigens in a HUVEC lysate (Fig. S4). In addition, anti-human IP-10, IFN-gamma, anti-MIG and anti-HMGBox1 reactivities were observed in Fe(II)-exposed IVIg using a BioPlex or ELISA assays, whereas native IVIg and pooled IgM preparations had no detectable antibodies to the studied cytokines. Antibodies to endogenous "danger" molecules - free Histone 3 and Histone 4, reported to possess a toxic effect on endothelial cells in sepsis (25), as well as to heat shock proteins were also present in the modified preparation (Table 1 and Fig. S5).

Discussion

Passive immunotherapy with commercially available therapeutic IVIg exposed *in vitro* to a low concentration of pro-oxidative ferrous ions, significantly improved survival in animals with experimental sepsis and aseptic SIRS. The same immunoglobulin preparations were not protective in their native form. The improved survival was accompanied by lower serum levels of pro-inflammatory cytokines, normalization of the coagulation time, diminished consumption of C3 complement component and attenuated organ injury or dysfunction. These multimodal effects strongly suggest that the ferrous-exposed IVIg has acquired novel biological properties. Pooled IVIg are highly polyspecific therapeutic preparations. Previous studies point that their exposure to Fe(II)-ions or to ROS, released in inflammation sites, amplify further this polyspecificity (15).

IVIg are known to suppress-the harmful effects of activated complement cascade components by preventing their binding to the respective receptors (26). In the fluid phase the IVIg with enhanced polyspecificity did not perturb the capacity of C1q to recognize IgG immune complexes. The latter is in agreement with previous studies, showing that even at high doses IVIg do not alter C1q binding and complement activation on sensitized sheep erythrocytes used as a model of cell-bound immune complexes (27). Therefore, the administration of Fe(II) ions-modified IVIg will not affect C1q functions during the early phase of defense against pathogens. Moreover, C1q binds better to the surface immobilized Fe(II) ions-modified IVIg (as a model of immune complex) than to the native IVIg, suggesting that the modified preparation could be more effective in opsonizing invading bacteria. When allowed to interact in a fluid phase with C1q Fe(II) ions-exposed IVIg inhibited the binding of C1q to surface-bound CRP, suggesting that attenuation of the complement activation on damaged host cells or on bacteria could result.

Since CRP levels are increased up to 50 fold in sepsis (28) the inhibition of its effector functions may be beneficial by reducing the ongoing inflammation. In our experiments the Fe(II) ions-modified IVIg also showed enhanced binding to C3a anaphylatoxin expected to result *in vivo* in its rapid neutralization and elimination.

The net beneficial effect of the blunted host response upon administration of IVIg with enhaced polyspecificity were reflected in less organ damage primarily in kidneys (Fig. S6). The transcriptome analysis showed a high variability between the individual animals suggesting that detection of the differential expression of particular genes might be a transitory phenomenon in a highly disordered (chaotic) gene network dynamics, characteristic of the septic state (29). For instance, some of the untreated septic animals clustered with the IVIG treated and some - with the modified IVIg. Nevertheless, the experiment showed detectable changes in the gene expression patterns, specific for the modified IVIg. A different set up with larger experimental groups will be necessary to trace these changes of the cascade ultimately dampening the genomic storm (Fig. S2).

The idea that polyspecific natural antibodies may act as a buffering system that prevents brisk changes in the levels of circulating cytokines, hormones, etc., has been proposed twenty years ago (30). The immune-suppressive properties of plasma during sepsis have been discussed extensively before. Diverse factors are currently considered in this context: IL-10, extracellular ubiquitin, circulating CD14, epinephrine and other inducible signals (31). Such a convergence of different activities towards an anti-inflammatory plasma compartment indicates the importance of this principle. It is thus not surprising that the quasi-complete repertoire of circulating natural antibodies can be conditionally recruited to that function too.

It is counter-intuitive that naturally polyspecific IgG antibodies should generally limit or block cytokine activities in the tissues. On the other hand, *in vivo* induced polyspecificity would be limited in space (to the site of inflammation) and time (IgG polyspecificity would result in a short half-life (32) and molecules gaining systemic access would be quickly diluted). Thus, its effect would be tightly controlled. It is possible that the *in vitro* treatment of IVIg with protein-destabilizing agents serendipitously activated this function on a large scale. Intravenous infusion of immunoglobulin preparation with additionally enhanced polyspecificity would apply systemically a “buffer” system that evolution have meant to have a local effect. During the event of uncontrolled systemic inflammation (sepsis) this may be helpful as it would enhance the inherent anti-inflammatory activity of plasma. Our data provide evidence to support this hypothesis as only the modified, but not the native IVIg preparation binds to a) a panel of antigens in a HUVEC lysate, b) mediators of inflammation – IFNγ, IP-10/CXCL10, MIG/CXCL9 and HGMB1, c) the complement components C1q and C3a, and d) the hydrophobic "danger signals" heat shock proteins and the free extracellular histones H3 and H4 (see Refs. (15, 25) and Figs. 3, S4 and S5). Importantly, our studies revealed that Fe(II) ions exposure is associated with considerable increase in the hydrophobicity of antigen binding sites of IgG (15). As endogenous danger signals have frequently hydrophobic nature, antibody-mediated non-specific quenching of hydrophobicity may also well explain the systemic anti-inflammatory effect of modified IVIg (33, 34).

Furthermore, the elimination of the formed immune complexes by Fc receptor-expressing phagocytes may contribute to the down-regulation of the ongoing severe generalized inflammatory reaction.

Although the dependence of the observed therapeutic effect of modified IVIg on lymphocytes and macrophages is compatible with the "immunosomatics" mechanism (30), an effect, mediated by a particular mononuclear cell population, cannot be ruled out. Innate response activator (IRA) $CD19^{low}CD5^{low}CD93^{+}$ B cells have been implicated recently in the control of experimental sepsis in mice (35). Indeed, our recent studies show that, unlike native IVIg, ferrous ions exposure-modified IVIg induced in the LPS-injected mice higher levels of IRA B cells and the beneficial effect of the treatment on survival correlated with this increase (36).

Conclusion

This work contains evidence that pleiotropic therapeutic approaches offer a viable strategy for treatment of sepsis and aseptic SIRS. Apart from the mechanistic explanation, the pleiotropy principle also justifies the use of mouse models despite the controversy on differences in transcriptome profiles in humans and mice with severe inflammatory syndromes (37, 38).

Acknowledgments

This work was supported by grants from the Bulgarian-Swiss Research Programme (BSRP IZEBZO_142967), the Bulgarian National Science Fund (DFNI B02/29), the Pasteur Institute (ACIP A07-2012), the NATO Science for Peace Program (SfP 982158), the German Federal Ministry of Education and Research (BMBF; grant 01EO1002) and grant 03Z2J521 (Meta-ZIK) - both to the Centre for Sepsis Control and Care. We thank D. Himsel for technical assistance.

For More Information The microarray data generated in this publication have been deposited in NCBI's Gene Expression Omnibus (GEO) and are accessible through the accession number GSE55964.

Competing financial interests

The authors declare competing financial interests: TV is applicant and TV and JD are inventors of a patent.

References:

1. Angus DC, van der Poll T. (2013) Severe sepsis and septic shock. N Engl J Med. 369:840-851.

2. Jean-Marc Cavaillon CAE (2008) Sepsis and Non-infectious Systemic Inflammation: from Biology to Critical Care, Weinheim: Wiley-VCH Verlag GmbH & Co.

3. The INIS Collaborative Group (2011) Treatment of Neonatal Sepsis with Intravenous Immune Globulin. N Eng J Med. 365:1201-1211.

4. Rittirsch D, Flierl MA, Ward PA. (2008) Harmful molecular mechanisms in sepsis. Nat Rev Immunol. 8:776-787.

5. Bouvet J, et al. (2001) Induction of natural autoantibody activity following treatment of human immunoglobulin with dissociating agents. J Autoimmun. 16:163-172.

6. Xiao W, et al. (2011) A genomic storm in critically injured humans. J Exp Med. 208:2581-2590.

7. Kazatchkine MD, Kaveri SV. (2001) Immunomodulation of Autoimmune and Inflammatory Diseases with Intravenous Immune Globulin. N Engl J Med. 345: 747-755.

8. Lutz HU. (2012) Naturally Occurring Antibodies (NAbs). Landes Bioscience, Austin, TX, USA.

9. Laupland KB, Kirkpatrick AW, Delaney A. (2007) Polyclonal intravenous immunoglobulin for the treatment of severe sepsis and septic shock in critically ill adults: A systematic review and meta-analysis*. Crit Care Med. 35:2686-2692.

10. Soares MO, et al. (2012) An evaluation of the feasibility, cost and value of information of a multicentre randomised controlled trial of intravenous immunoglobulin for sepsis (severe sepsis and septic shock): incorporating a systematic review, meta-analysis and value of information analysis. Health Technology Assessment. 16:1-18611.

11. Werdan K, et al. (2007) Score-based immunoglobulin G therapy of patients with sepsis: The SBITS study. Critical Care Medicine. 35:2693-2701.

12. Djoumerska I, Tchorbanov A, Pashov A, Vassilev T. (2005) The autoreactivity of therapeutic intravenous immunoglobulin (IVIG) preparations depends on the fractionation methods used. Scand J Immunol. 61:357-363.

13. Djoumerska-Alexieva IK, et al. (2010) Exposure of IgG to an acidic environment results in molecular modifications and in enhanced protective activity in sepsis. FEBS J. 277:3039-3050.

14. Pavlovic S, et al. (2011) Intravenous immunoglobulins exposed to heme (heme IVIG) are more efficient than IVIG in attenuating autoimmune diabetes. Clin Immunol. 138:162-171.

15. Dimitrov JD, et al. (2006) Ferrous ions and reactive oxygen species increase antigen-binding and anti-inflammatory activities of immunoglobulin G. J Biol Chem. 281:439-446.

16. Dimitrov J, et al. (2007) Antibodies use heme as a cofactor to extend their pathogen-eliminating activity and to acquire new effector functions. J Biol Chem. 282:26696-26706.

17. McIntyre J, Wagenknecht D, Faulk W. (2006) Redox-reactive autoantibodies: detection and physiological relevance. Autoimmun Rev.5:76.

18. Djoumerska-Alexieva IK, Dimitrov JD, Nacheva J, Kaveri SV, Vassilev TL. (2009) Protein destabilizing agents induce polyreactivity and enhanced immunomodulatory activity in IVIg preparations. Autoimmunity. 42:365-367.

19. Hubbard WJ, et al. (2005) Cecal ligation and puncture. Shock. 24 Suppl 1:52-57

20. Volman TJ, Hendriks T, Goris RJ. (2005) Zymosan-induced generalized inflammation: experimental studies into mechanisms leading to multiple organ dysfunction syndrome. Shock. 23:291-297.

21. Ivanovska ND, et al. (2008) Properdin deficiency in murine models of nonseptic shock. J Immunol. 180:6962-6969.

22. Haeffner-Cavaillon N, Klein M, Dorrington KJ. (1979) Studies on the Fc gamma receptor of the murine macrophage-like cell line P388D1. I. The binding of homologous and heterologous immunoglobulin G1. J Immunol. 123:1905-1913.

23. Ward PA, Gao H. (2009) Sepsis, complement and the dysregulated inflammatory response. J Cell Mol Med. 13:4154-4160.

24. Markiewski MM, DeAngelis RA, Lambris JD. (2008) Complexity of complement activation in sepsis. J Cell Mol Med. 12:2245-2254.

25. Xu J, et al. (2009) Extracellular histones are major mediators of death in sepsis. Nat Med. 15:1318-1321.

26. Basta M. (2008) Ambivalent effect of immunoglobulins on the complement system: activation versus inhibition. Mol Immunol. 45:4073-4079.

27. Basta M, Fries LF, Frank MM. (1991) High doses of intravenous Ig inhibit in vitro uptake of C4 fragments onto sensitized erythrocytes. Blood. 77:376-380.

28. Devran O, et al. (2012) C-reactive protein as a predictor of mortality in patients affected with severe sepsis in intensive care unit. Multidiscip Respir Med. 7:47-52.

29. Tang BM, Huang SJ, McLean AS. (2010) Genome-wide transcription profiling of human sepsis: a systematic review. Crit Care 14: R237.

30. Coutinho A, Avrameas S. (1992) Speculation on immunosomatics : Potential diagnostic and therapeutic value of immune homeostasis concepts. Scand J Immunol. 36:527-532.

31. Cavaillon JM, Adib-Conquy M. (2007) Determining the degree of immunodysregulation in sepsis. Contrib Nephrol. 156:101-111.

32. Sigounas G, Harindranath N, Donadel G, Notkins AL. (1994) Half-life of polyreactive antibodies. J Clin Immunol. 14:134-140.

33. Matzinger P. (2002) The danger model: a renewed sense of self. Science. 296:301-305.

34. Seong SY, Matzinger P. (2004) Hydrophobicity: an ancient damage-associated molecular pattern that initiates innate immune responses. Nat Rev Immunol 4**:**469-478.

35. Rauch PJ, et al. (2012) Innate response activator B cells protect against microbial sepsis. Science. 335:597-601.

36. Djoumerska-Alexieva I, Pashova S, Vassilev T, Pashov A. (2013) The protective effect of modified intravenous immunoglobulin in LPS sepsis model is associated with an increased IRA B cells response. Autoimmun Rev. 12:653-656.

37. Seok J, et al. (2013) Genomic responses in mouse models poorly mimic human inflammatory diseases. PNAS 110:3507-3512.

38. Takao K, Miyakawa T. (2015) Genomic responses in mouse models greatly mimic human inflammatory diseases. PNAS 112:1167-1172.

Table 1. Exposure of IVIg to ferrous ions results in the appearance of reactivity to some of the tested human cytokines, complement components and "danger" molecules. Antibody reactivity to mouse IFN-γ were measured in a control ELISA experiment. NS* - not shown.

	Inflammation-related and "danger" molecules	Binding appears after IVIg exposure to ferrous ions	Method used	Reference
	Cytokines			
1	MIG	Yes	ELISA	Fig. S5
2	IP-10	Yes	BioPlex Array	Fig. S5
3	HMGB1	Yes	ELISA	Fig. S5
4	IFN-γ	Yes	BioPlex Array	Fig. S5 and Ref.15
5	Mouse IFN-γ	No	ELISA	Fig. S5
6	IL-8	No	BioPlex Array	NS
7	IL-10	No	BioPlex Array	NS
8	IL-15	No	BioPlex Array	NS
9	G-CSF	No	BioPlex Array	NS
10	MCP-1	No	BioPlex Array	NS
11	MIP-α	No	BioPlex Array	NS
12	MIP-β	No	BioPlex Array	NS
13	TNF-α	No	BioPlex Array	Fig. S5
14	IL-6	No	ELISA	NS
15	IL1-RA	No	ELISA	NS
16	RANTES	No	BioPlex Array	NS
	Complement components			
17	C1q	Yes	ELISA	Fig. 3B
18	C3a	Yes	ELISA	Fig. 3D
19	C5a	No	ELISA	Fig. 3D
	"Danger" molecules			
20	Histone 3	Yes	ELISA	Fig. S5
21	Histone 4	Yes	ELISA	NS
22	HSP 60	Yes	ELISA	Fig. S5
23	HSP 70	Yes	ELISA	Fig. S5
24	HSP 90	Yes	ELISA	NS

Figure legends:

Figure 1. Passive immunotherapy with IVIg modified by Fe(II) exposure improves animal survival in two aseptic SIRS and one polymicrobial sepsis models. Outbred female ICR mice were used in the experiments. (A) Endotoxemia was induced by the i.p. injection of 10 mg/kg *E. coli* LPS (left panel). Zymosan-induced systemic inflammation (middle panel) was caused by i.p. injection of 500 mg/kg zymosan. Polymicrobial CLP-induced sepsis (right panel) was performed as described in the Materials and methods section. The survival was compared between the control group, injected i.v. with PBS (open squares, n = 12), the group with endotoxemia treated with 50 mg/kg or of 250 mg/kg (in zymosan-induced inflammation and CLP sepsis) native IVIg (triangles, n = 12), and a group treated with 50 mg/kg (endotoxemia) or 250 mg/kg (zymosan-induced inflammation and CLP sepsis) Fe(II)-exposed IVIg (circles, n = 12); *$p<0.05$, Mantel-Haenszel logrank test). (B) The beneficial effect of the Fe(II)-exposed preparation on survival was still observed if its administration was delayed. Endotoxemia was induced as described above and the mice were treated i.v. with 50 mg/kg of the native (open bars) or Fe(II)-exposed IVIg (black bars) at different time points – minutes before, one, or four hours after the i.p. injection of LPS. (C) Residual iron ions in Fe(II)-exposed IVIg did not contribute to its protective effect in LPS sepsis. ICR mice (n=12) were injected i.p with 10 mg/kg E. coli LPS and treated i.v. with 50 mg/kg Fe(II)-exposed IVIg with high (7.2 mg/g IgG, black circles) or low (0.66 mg/g IgG, white circles) iron concentration or with PBS only (open squares).

Figure 2. Serum levels of inflammation-related molecules in treated endotoxemic mice. (A) Endotoxemia was induced by the i.p. injection of 10 mg/kg *E. coli* LPS. A control group was

injected i.v. with PBS (*n* = 10, light grey bars), a second group was injected i.v. with 50 mg/kg of native IVIg (n = 10, dark grey bars), and a third group - with 50 mg/kg of Fe(II)-exposed IVIg (n=10, black bars). Cytokine levels in untreated mice are represented with white bars. Sera were obtained 4, 24 and 48 h after LPS injection and cytokine levels were measured by ELISA. Data represent mean pg/ml values±SD of quadruplicate wells, *p<0.05 (paired Student *t*-test). (B) Scan of dot blots evaluating semi-quantitatively of serum levels of a larger panel of inflammatory molecules two hours after LPS injection. Each blot is representative of three individual experiments. (C) The individual dots (see panel B) were subjected to densitometry and the data were analyzed using the Image-Tool v2.0 for Windows (UTHSCSA, San Antonio, TX, USA) software package and were represented in relative units of grey intensity (n=3, mean±SD, *p<0.05, paired Student *t*-test).

Figure 3. A single administration of Fe(II) exposure-modified IVIg overcomes the coagulation and complement abnormalities in LPS-induced sepsis. (A) Endotoxemia was induced to ICR mice by the i.p. injection of 10 mg/kg *E. coli* LPS. A control group (n=10, open squares) was injected i.v. with PBS, a second group was treated with 50 mg/kg native IVIg (n = 10, black triangles), and a third was treated with 50 mg/kg Fe(II)-exposed IVIg (n=10, black circles). Serum samples were collected at 4, 24 and 48 hour after LPS administration and the C3 levels in plasma were measured using a commercial Mouse C3 ELISA kit, *p<0.05, paired t-test. (B) The exposure of IVIg to Fe(II)-ions results in its increased binding to C1q molecules (black circles) compared to that of native IVIg (black triangles), mean±SD**.** (C) C1q pretreatment with Fe(II)-exposure modified IVIg inhibits the binding of the former to CRP (black circles); in comparison to C1q pretreated with native IVIg (black triangles). The binding of untreated C1q is

presented with open squares. (D) The exposure of IVIg to increasing concentrations of ferrous ions results in an enhanced binding to the C3a, but not the C5a component Anti-C3a and anti-C5a reactivity was compared by ELISA in IVIg, exposed to increasing concentrations of ferrous ions. (E) Endotoxemia was induced to ICR mice by the i.p. injection of 10 mg/kg *E. coli* LPS. A control group was treated i.v. with PBS (n=10, light grey bars), a group was treated with 50 mg/kg native IVIg (n = 10, dark grey bars), and another was treated with 50 mg/kg Fe(II)-exposed IVIg (n=10, black bars). Animals were bled 4 hours after the injection of LPS and coagulation time was measured as previously described (*21*), *p<0.05; ***p<0.001, *t*-test. (F) Bilirubin serum levels measured four hours after LPS administration in groups of mice treated with native (n=10, dark grey bars), Fe(II) -exposed IVIg (n=10, black bars) or PBS alone (n=10, light grey bars). *p<0.05, *t*-test.

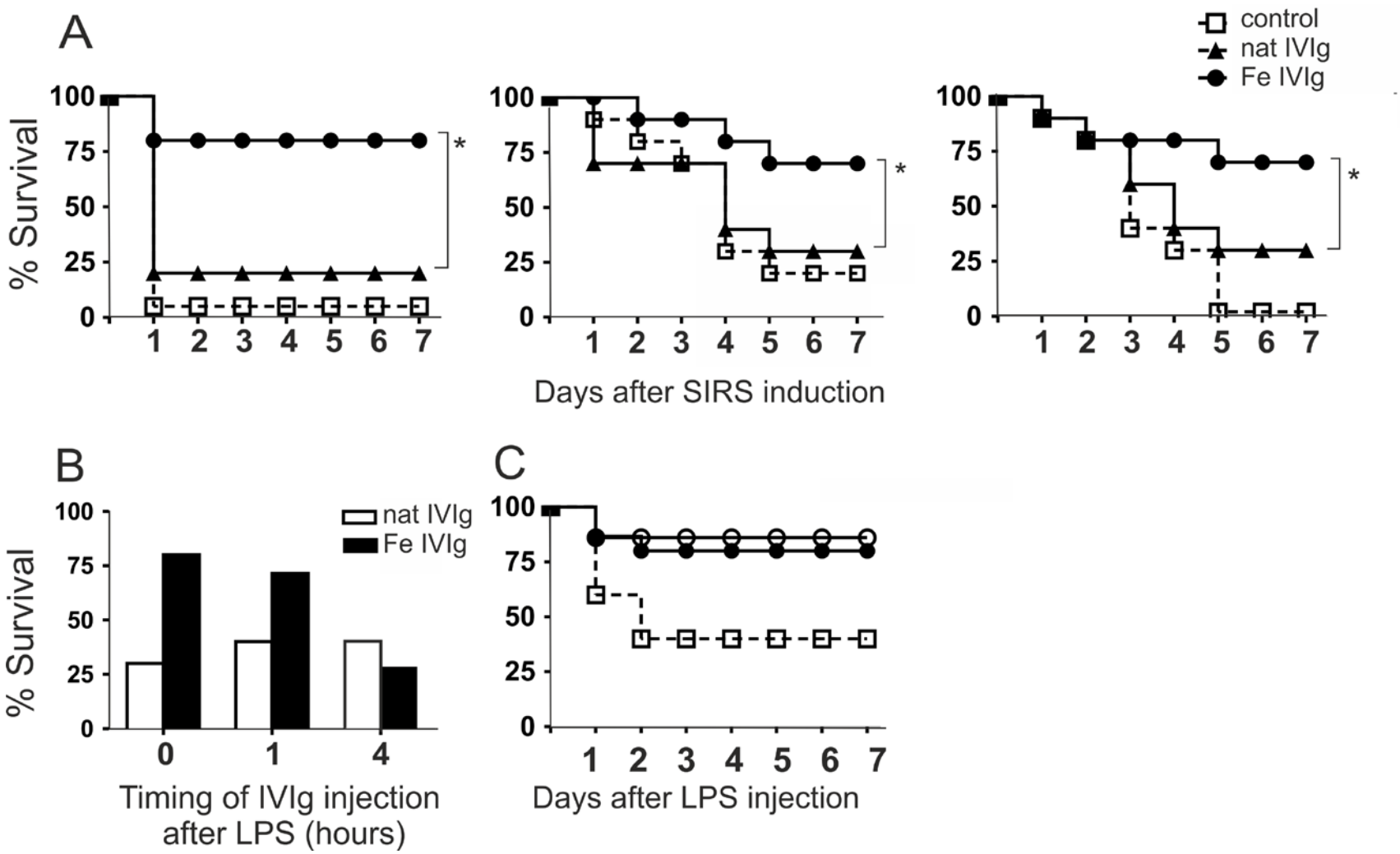

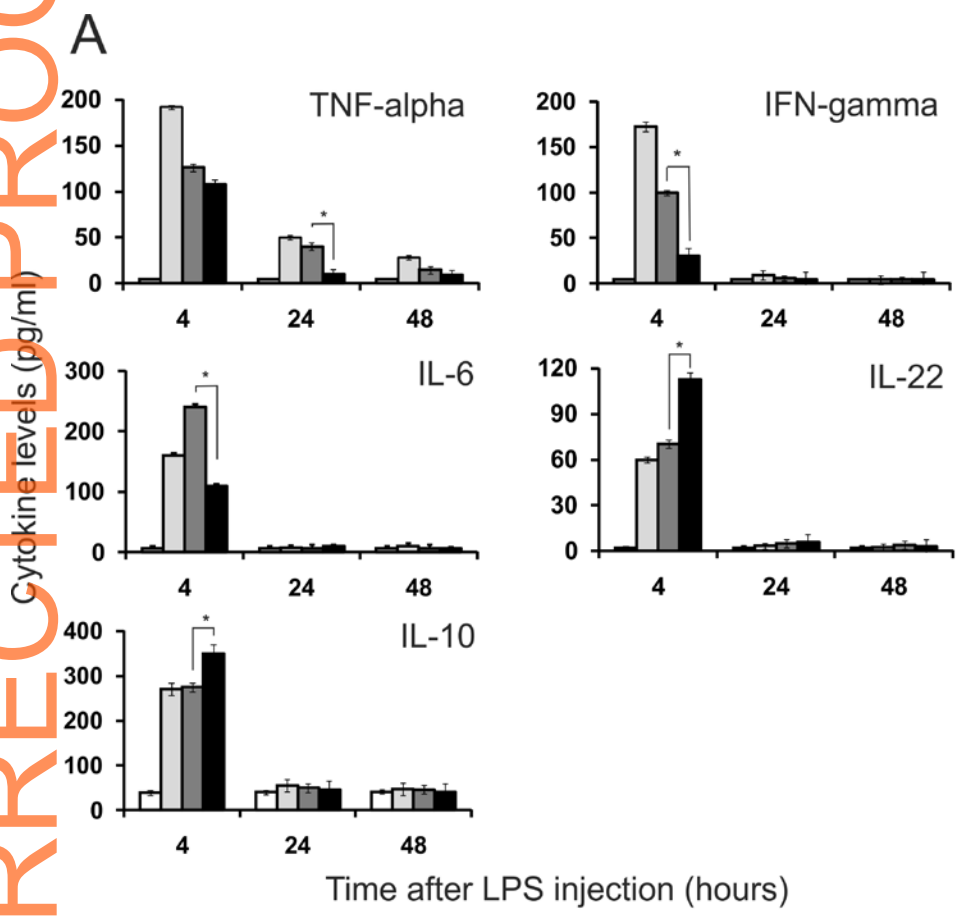

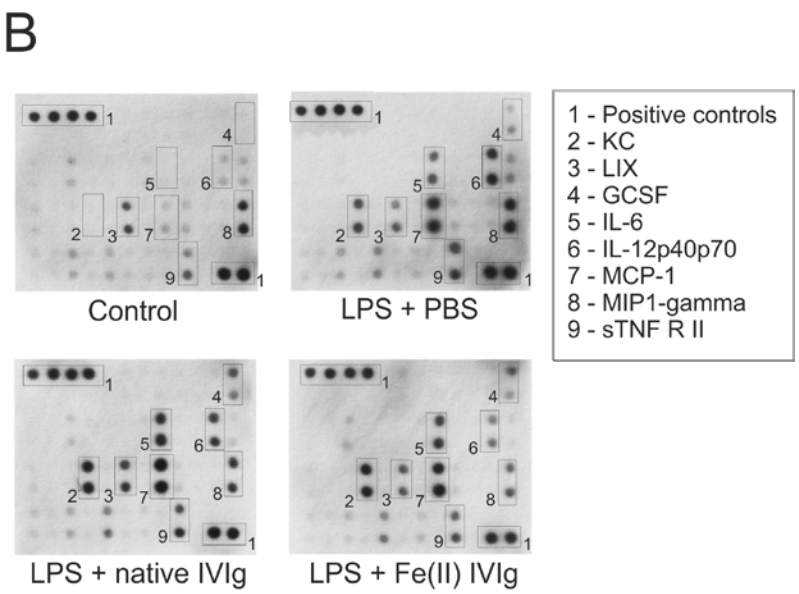

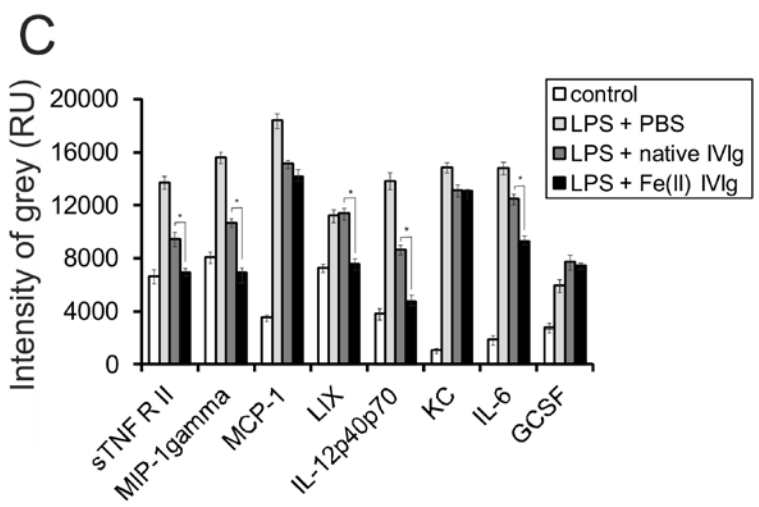

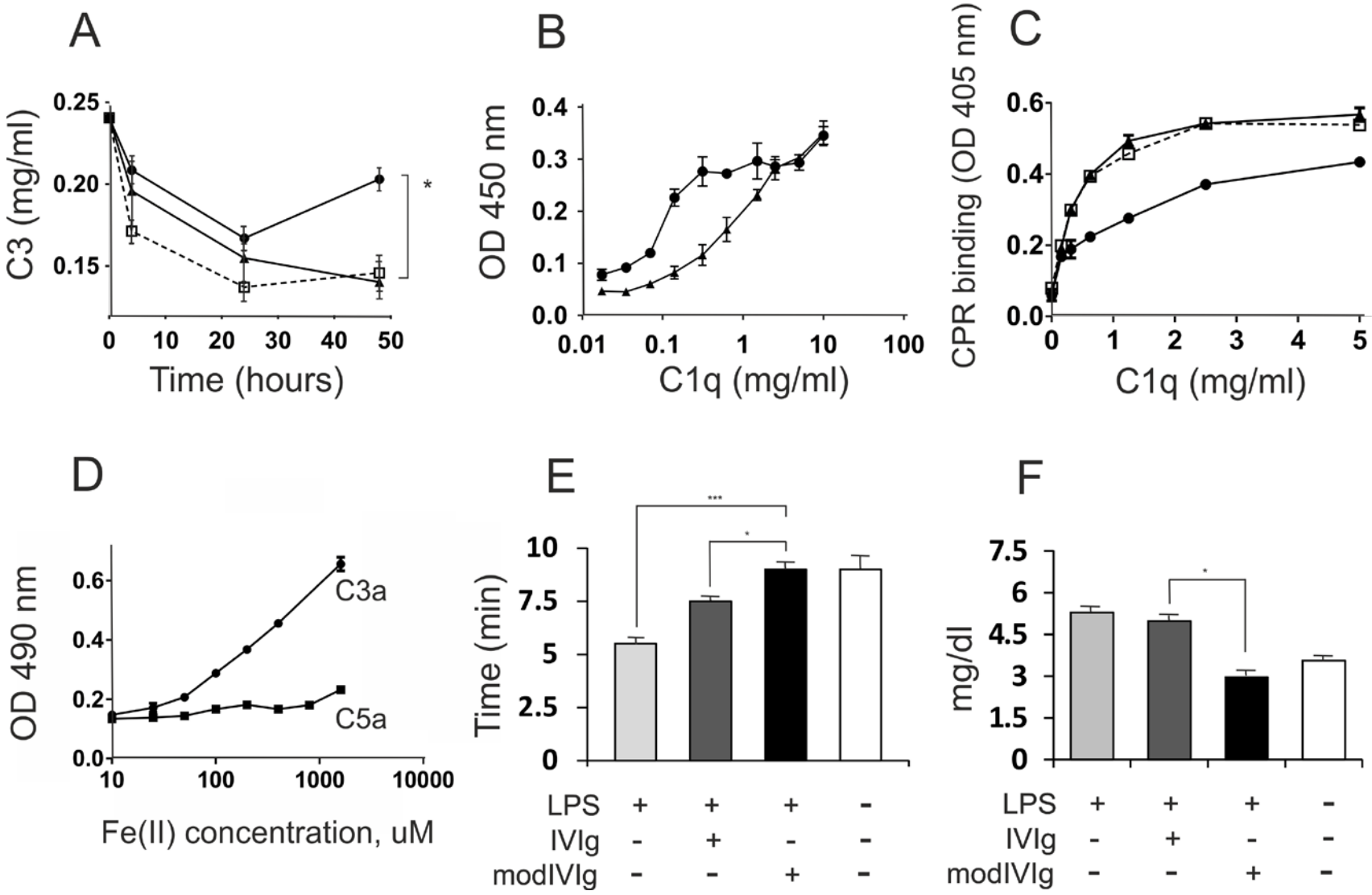

Supporting information:

Materials and Methods

Flame atomic absorption spectroscopy

The concentration of iron ions in the IVIg preparations under study was measured by flame atomic absorption spectrometry. The samples were diluted 1:2 with a 20% (W/V) trichloro acetic acid solution, and heated in a heating block for 15 minutes at 90°C. They were next cooled, centrifugated and the iron concentration was determined using a Perkin Elmer M 5000 atomic absorption spectrometer.

Gene expression analysis

C57Bl/6 mice were used in this analysis. Blood samples, liver and kidney homogenates were obtained and processed by standard protocols. RNA was extracted using the RNeasy minikit (Qiagen, Hilden, Germany) in a balanced design comprising three biological replicates from blood and four from liver and kidney of each treatment group (vehicle, native IVIg, Fe(II)-exposed IVIg) respectively. Biotinylated probes were prepared using the TargetAmp™-Nano Labeling Kit for Illumina® Expression BeadChip® (Illumina, San Diego, CA). The arrays were scanned using the Illumina BeadArray Reader 500 X.

Illumina mouseRef8 V2 chips were read by Genome Studio (v.1.9, and annotation MouseRef-8_V2_0_R3_11278551_A) yielding 25,697 bead probes for each sample. Analysis was performed consistently using R software version 3.02 (http://www.r-project.org/) and Bioconductor (1) packages. Raw data from each organ was separately subjected to robust spline normalization, quality control and background correction with the R package Lumi (2). Two samples (one from blood cells, one from kidney) did not pass quality control and were discarded from analysis. Bead types having detection values $p < 0.05$ of the RNA samples

were called "present" and taken for further analysis. Differentially expressed genes (DEG) were filtered according to microarray quality control criteria (MAQC, (3)) by: 1) at least two-fold changes and 2) p-values from moderated t-statistics <0.05 using ”Limma” (24). Further, these statistics were computed for all the contrasts (IVIg, Fe(II) exposure-modified IVIg (modIVIg), vehicle) using linear model fits, moderated t-and F-statistics, and log-odds of differential expression by empirical Bayes moderation. Gene set enrichment analysis was performed by hypergeometric tests with the WebGestalt tool (4). Annotation, log2 fold changes, top enriched categories and p-values are provided as Supplemental gene expression data.

Binding of and modified IVIg to bacterial lipopolysaccharide

ELISA plates were coated with *E. coli* LPS (B 055:B5, Sigma #L2880, at 5 ug/ml in PBS) and blocked. Serial dilutions of the IVIg preparations were added in triplicate wells and the binding of the pooled human IgG was measured by ELISA.

In a separate experiment the native- and the Fe(II)-exposed IVIg were mixed in the wells of a blocked ELISA plate with increasing concentrations of *E.coli* LPS and incubated for two hours at room temperature. These mixtures were transferred to a second LPS-coated plate and the binding of human IgG was measured by ELISA as described in the Methods section. Its inhibition in the presence of free LPS was determined and presented in arbitrary units.

Immunoblot analysis of binding to HUVEC antigens

HUVEC cells lysates were subjected to 10% gel SDS-PAGE and transferred to nitrocellulose membranes (Scheicher & Schuell, Dassel, Germany) by a Mini Transfer Blot system (BioRad, Richmond, CA). Next, the membranes were incubated for 1 hour at room temperature in TBS containing 0,4% Tween 20, cut into strips and incubated for 1 h at room

temperature with native or Fe(II)-exposed IVIg preparations at concentrations of 0,2 mg/ml. After extensive washing the strips were incubated with an anti-human IgG antibody (Fc-specific), conjugated to alkaline phosphatase (Sigma Chemical Co, St. Louis, MO) and revealed using the nitro blue tetrazolium/bromo-chloro-indolyl-phosphate substrates (Sigma).

Antibodies to pro-inflammatory and "danger" molecules in the modified IVIg

The presence of antibodies to cytokines, complement components and "danger" molecules was studied using ELISA and BioPlex Array (see the Materials and Methods section of the main text).

Histology

ICR mice (8-12 weeks old, 18-22 g) were used in this experiment. Endotoxemia was induced by the i.p. injection of 10 mg/kg *E. coli* LPS (B 055:B5, #L2880, Sigma-Aldrich St. Luis, MO). Single dose of native, modified IVIg preparations or PBS alone was injected intravenously (i.v.) 10 min before the administration of LPS. Kidneys and livers from each experimental group were collected 24 h after the injection of LPS. The organs were fixed in 4% buffered formalin, embedded in paraffin, sectioned into 3.5 µm thick slices and stained with Hematoxylin and Eosin (H&E). Pathologists blinded for the treatments estimated kidney damage in mice challenged with LPS + vehicle (n=8), LPS + native IVIg (n=10), LPS + Fe(II)-exposed IVIg (n=10) using the following criteria: the presence of brush-border defects, flattening of epithelia, loss of nuclei and presence of debris all indicative of an acute tubular injury (ATI) (5). Presence of liver damage was graded based on sinusoidal congestion, nuclear and cytoplasmic irregularities, signs of cellular ischemia, sinusoidal infiltration and single cell necrosis (6).

Table S1. The concentration of iron in the studied immunoglobulin preparations was measured by atomic absorption spectrometric analysis.

Preparation	Iron concentration
Native (untreated) IVIg	0.028 mg/g IgG
Fe(II)-exposed IVIg	7.2 mg/g IgG
Fe(II)-exposed IVIg dialyzed additionally against 4mM EDTA	0.66 mg/g IgG

Figure legends:

Figure S1. Reduced mortality in three different experimental models of sepsis after passive immunotherapy with an IVIg preparation, modified by Fe(II) exposure. (A) Survival curves of ICR mice with bacterial LPS-induced endotoxemia. Animals were injected i.p. with 10 mg/kg *E. coli* LPS. A survival study was performed comparing a control group, treated i.v. with PBS (open squares, *n* = 12), a group treated with 2 mg/kg (left panel), 10 mg/kg (middle panel) or 50 mg/kg (right panel) native IVIg (triangles, *n* = 12), and a group treated with 2 mg/kg (left panel), 10 mg/kg (middle panel) or 50 mg/kg (right panel) Fe(II)-exposed IVIg (circles, *n* = 12); *p<0.05, Mantel-Haenszel logrank test). (B) Survival curves of ICR mice with zymosan-induced systemic inflammation. Animals were injected i.p. with 500 mg/kg zymosan. A survival study was performed comparing a control group, treated i.v. with PBS (open squares, *n* = 12), a group treated with 10 mg/kg (left panel), 50 mg/kg (middle panel) or 250 mg/kg (right panel) native IVIg (triangles, *n* = 12), and a group treated with 10 mg/kg (left panel), 50 mg/kg (middle panel) or 250 mg/kg (right panel) Fe(II)-exposed IVIg (circles, *n* = 12); *p<0.05, Mantel- Haenszel logrank test). (C) Survival curves of ICR mice with polymicrobial CLP-induced sepsis. Survival was compared between a control group, injected i.v. with PBS (open squares, *n* = 12), a group treated with 10 mg/kg (left panel), 50 mg/kg (middle panel) or 250 mg/kg (right panel) of native IVIg (triangles, *n* = 12), and a group treated with 10 mg/kg (left panel), 50 mg/kg (middle panel) or 250 mg/kg (right panel) of Fe(II)-exposed IVIg (circles, *n* = 12). *p<0.05, Mantel- Haenszel logrank test).

Figure S2. Blood cell, liver and kidney gene expression in LPS-injected mice treated with native- or Fe(II)-exposed IVIg (modIVIg). Heatmaps depicting the differentially expressed genes (DEG, average two-fold change and p<0.05) for Fe(II)-exposed IVIg versus

native IVIg in blood (A), liver (B) and kidney (C), respectively. Resolved log2 signals of biological replicates were row-wise scaled (z-score) accompanied by vertical and horizontal hierarchical correlation clustering (technical probe replicates are indicated by ".1". Definition of gene symbols is provided in the supplement files. The Venn diagrams depict the number of DEG for all contrasts (D).

Figure S3. The exposure of IVIg to ferrous ions does not affect its binding to LPS. (A) Increasing concentrations of native- and Fe(II)-exposed IVIg preparations (marked with squares and circles respectively) were left to interact with immobilized LPS and human IgG binding was evaluated by ELISA. (B) Both preparations were pre-incubated with increasing concentrations of LPS and the mixtures were transferred to the LPS-coated wells. Next, the binding of human IgG was measured by ELISA and its inhibition (presented in arbitrary units - AU) was plotted against the concentration of free LPS used.

Figure S4. Exposure of IVIg to increasing concentrations of Fe(II) ions results in its enhanced binding to antigens in a HUVEC lysate. The membranes were incubated with 200 µg/ml of the native IVIg or of the same preparation exposed to ferrous ions.

Figure S5. Ferrous ions-exposed IVIg acquires the ability to bind to various human pro-inflammatory molecules. The figure presents several examples whereas all results are showed in Table 1 of the main text. Reactivity to IFN-γ , IP−10 and TNFα were measured using BioPlex Array and in all other cases ELISA was used (see the Materials and Methods section of the main text). In a control experiment the reactivities of both studied preparations to mouse IFN-γ (mIFN-γ) were compared. The pie-chart summarizes all data and points out that modified IVIg acquires the ability bind to almost half of the unselected tested inflammation-related molecules.

Figure S6. Tissue damage score from histological specimen (kidney - A and B, liver - C and D) from mice with endotoxemia treated with native or Fe(II)-exposed IVIg. Kidney injury was evaluated by the presence of brush-border defects, flattening of epithelia, loss of nuclei and presence of debris, summarized in the acute tubular injury (ATI) score (1). Liver damage scoring was based on sinusoidal congestion, nuclear and cytoplasmic irregularities, signs of cellular ischemia, sinusoidal infiltration and single cell necrosis. Summaries are provided in A and C for kidney and liver, respectively. *$p<0.05$, *t*-test (Welch-modified, accounting for differences in variances) Fe(II)-exposed IVIg vs the other groups given in parametric plots.

References

1. Gentleman RC, et al. (2004) Bioconductor: open software development for computational biology and bioinformatics. Genome Biol 5:R80.

2. Du P, Kibbe WA, Lin SM. (2008) lumi: a pipeline for processing Illumina microarray. Bioinformatics 24:1547-1548.

3. Shi L, et al. (2006) The MicroArray Quality Control (MAQC) project shows inter- and intraplatform reproducibility of gene expression measurements. Nat Biotechnol 24:1151-1161.

4. Wang J, Duncan D, Shi Z, Zhang B. (2013) WEB-based GEne SeT AnaLysis Toolkit (WebGestalt): update 2013. Nucleic Acids Res 41:W77-83.

5. Bockmeyer CL, et al. (2011) ADAMTS13 activity is decreased in a septic porcine model. Significance for glomerular thrombus deposition. Thromb Haemost 105:145-153.

6. Recknagel P, et al. (2013) Mechanisms and functional consequences of liver failure substantially differ between endotoxaemia and faecal peritonitis in rats. Liver Int 33:283-293.

7. Smyth GK. (2004) Linear models and empirical bayes methods for assessing differential

expression in microarray experiments. Stat Appl Genet Mol Biol 3:Article3.

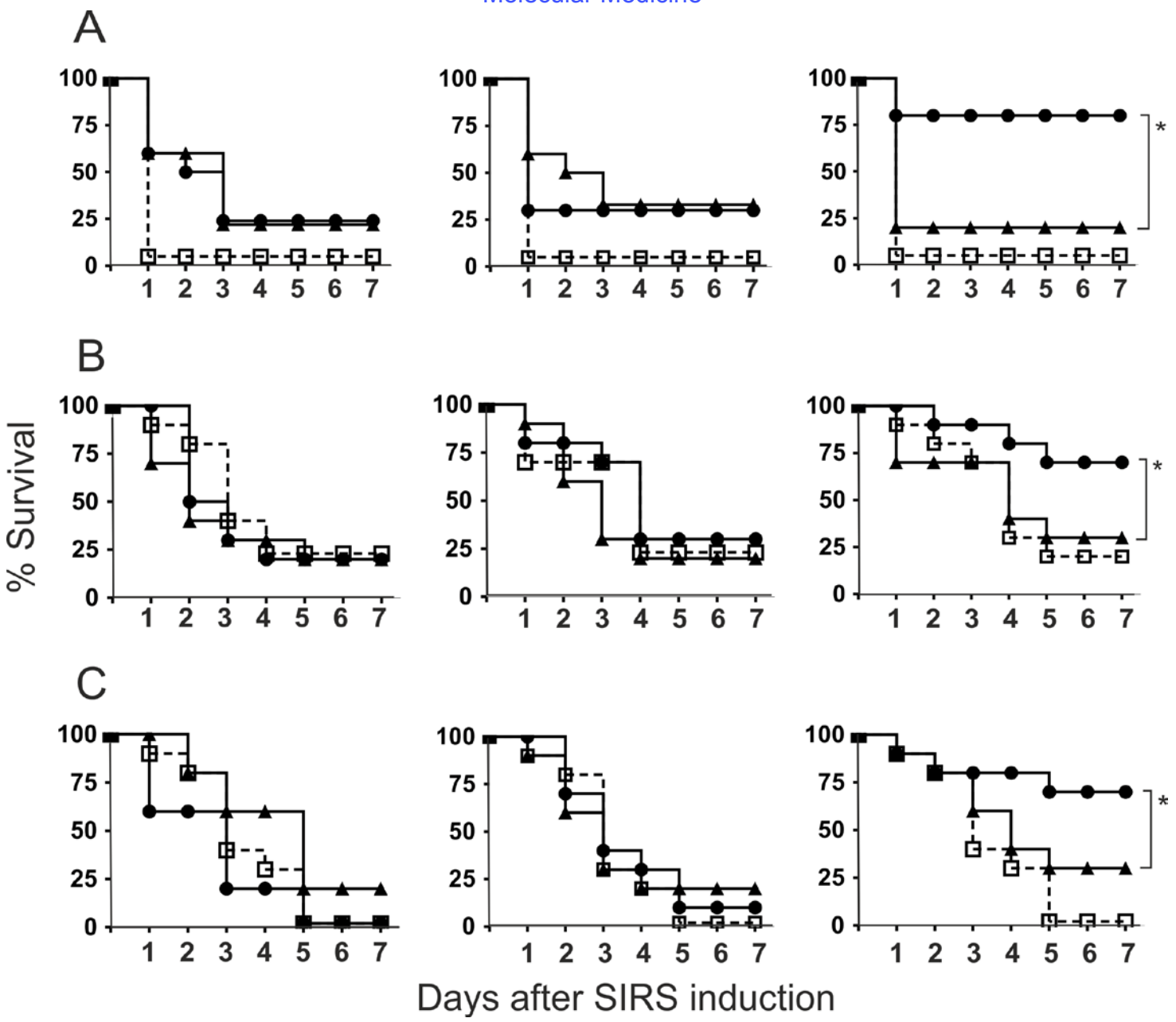

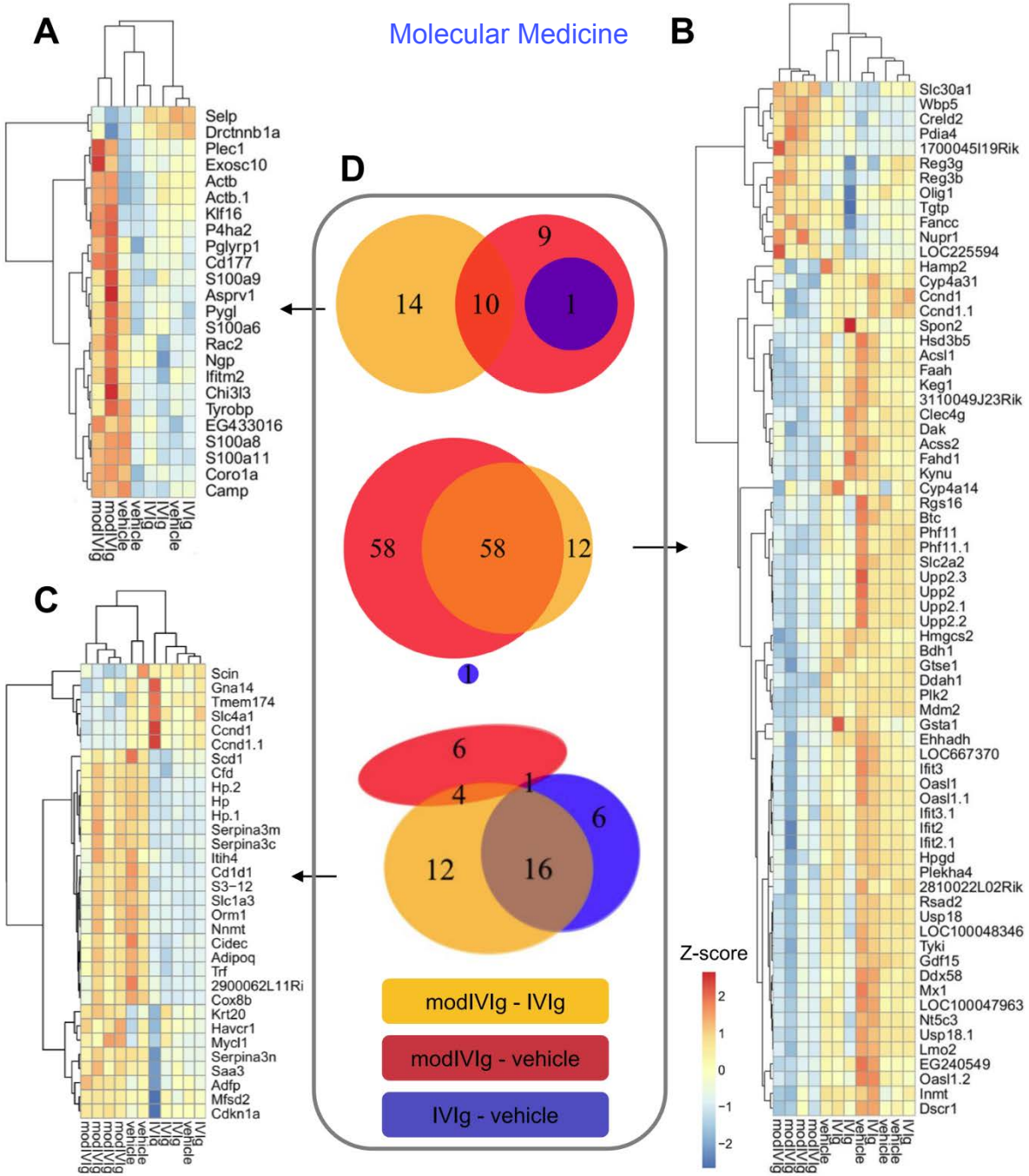

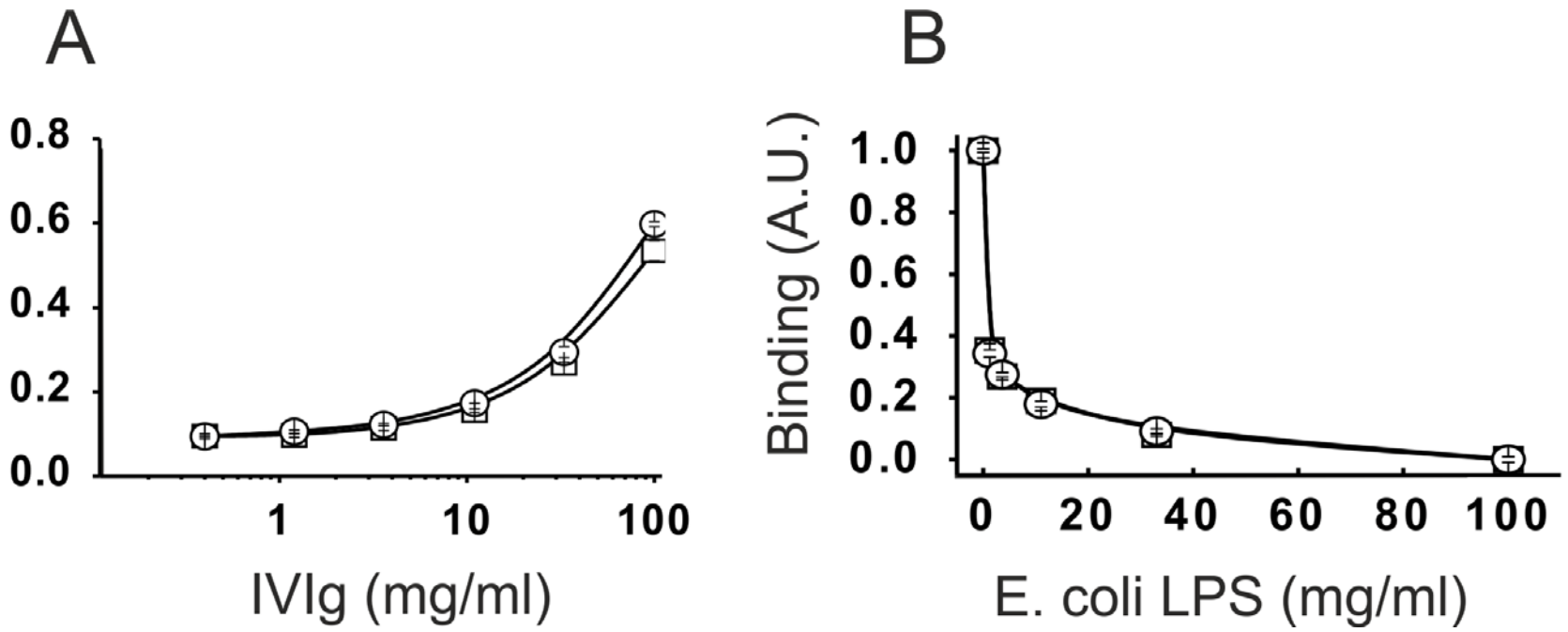

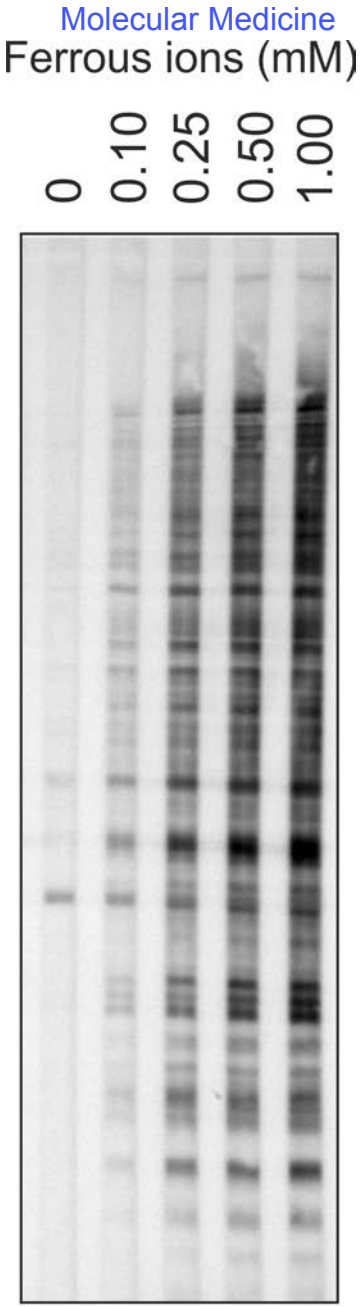

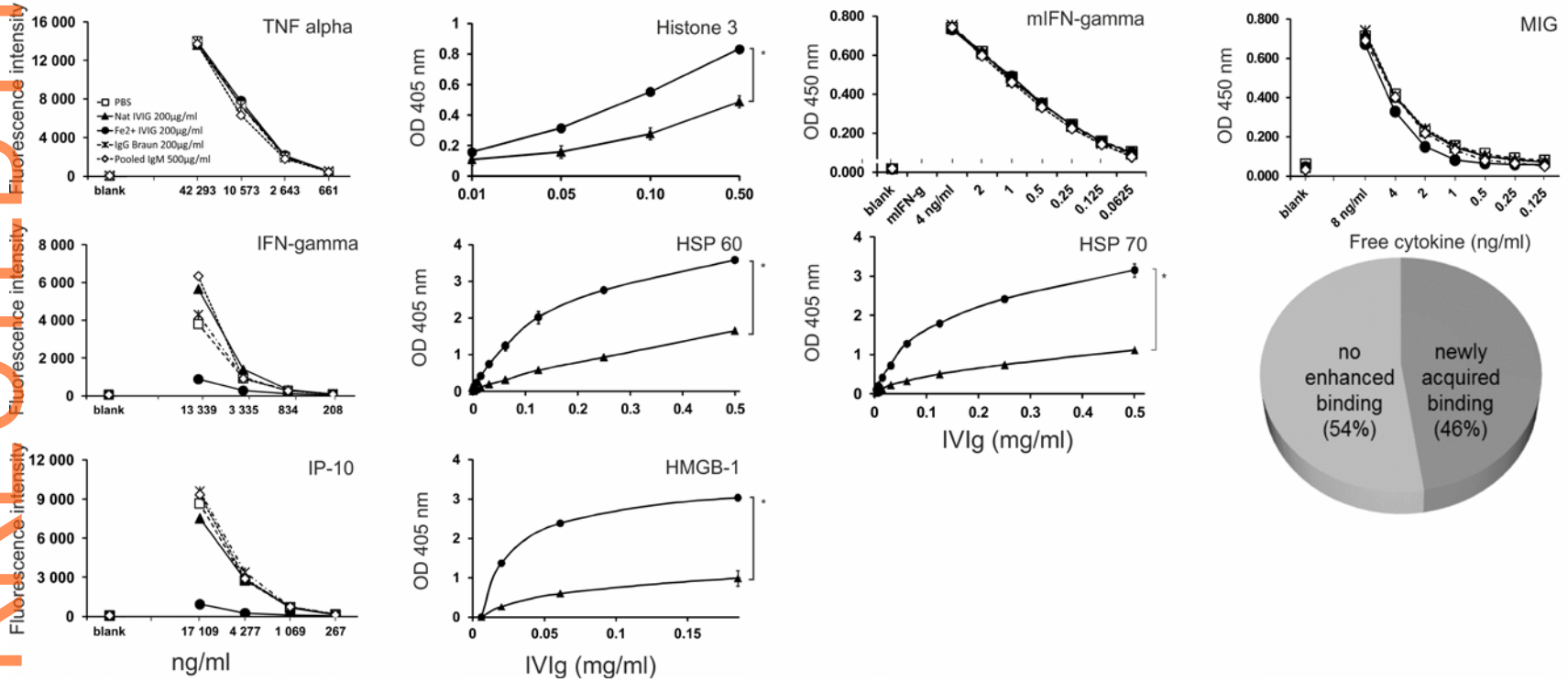

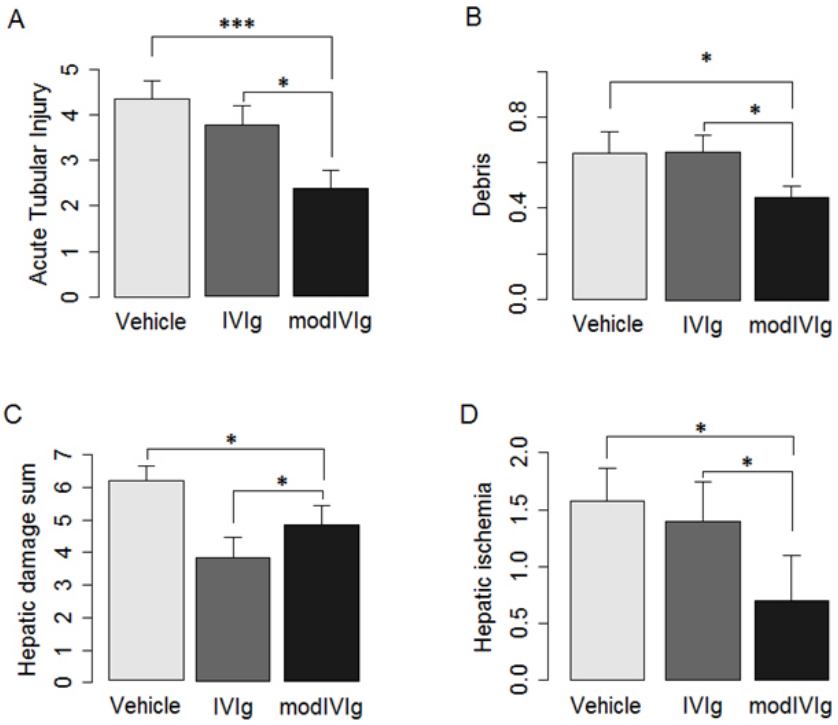

ILMN_Gene	average log2FC	IVIg-Vehicle	modIVIg-Vehicle	modIVIg-IVIg	P (moderated t-statistics)	IVIg-Vehicle	modIVIg-Vehicle	modIVIg-IVIg	Probe_Id	Probe_Sequence	Definition
2900062L11RIK		-1.416697695	-0.173654787	1.243042908		0.037431	0.775410146	0.0463929	ILMN_2609182	CCTTGTAGGTCCACATTGAATGCCGTTTTCTTATATCTTCTAGGGTGTGT	Mus musculus RIKEN cDNA 2900062L11 gene (2900062L11Rik), non-coding RNA.
ADFP		-0.594814157	0.717284553	1.31209871		0.0968802	0.051508139	0.00135786	ILMN_1222246	AGAAAATTCAGGGTGCTCAGGATAAGCTCTATGTCTCGTGGGTGGAGTG	Mus musculus adipose differentiation related protein (Adfp), mRNA.
ADIPOQ		-2.400097295	0.232938434	2.633035729		0.011571	0.771813749	0.00439888	ILMN_2738082	GACTGCAACTACCCATAGCCCATACACCAGGAGAATCATGGAACAGTCG	Mus musculus adiponectin, C1Q and collagen domain containing (Adipoq), mRNA.
AOC3		-1.531980725	-0.312202827	1.219777897		0.0366476	0.63477318	0.06509666	ILMN_2625920	GAGAGGGAATCAGGTTCTGCCTGCCCTTCTGAACATCATGGATTGGAAC	Mus musculus amine oxidase, copper containing 3 (Aoc3), mRNA.
APOC1		-1.299479683	-0.347932302	0.951547381		0.0479402	0.560706361	0.10537082	ILMN_2599794	AAAGTGAAGGAGAAGTTGAAGACCACGTTCTCCTGAGCACCTGGCGGG	Mus musculus apolipoprotein C-I (Apoc1), mRNA.
AQP4		-1.01024592	-1.330365875	-0.320119956		0.0777703	0.026900839	0.51716872	ILMN_2757232	GTGCAGAGCATATGGACACCTCTGTGAGGAAGCTGGCATTGTCCATCG	Mus musculus aquaporin 4 (Aqp4), mRNA.
CAR3		-1.362158574	-0.203605447	1.158553127		0.0381835	0.729427688	0.05319186	ILMN_2630047	CCCTGGCTCTGCTAAGACCATCCTGAACAATGGGAAGACCTGCAGAGT	Mus musculus carbonic anhydrase 3 (Car3), mRNA.
CCND1		0.381308916	-0.86206292	-1.243371836		0.3771588	0.062804125	0.00844535	ILMN_2601471	GCCATAGACTGGTGGTGGGTCCACGGAATCTGCCCTGTGACATGAAAGGC	
CCND1		0.398618927	-0.770912202	-1.169531129		0.3564935	0.090707034	0.01173754	ILMN_1221503	GGCCATAGACTGGTGGTGGGTCCACGGAATCTGCCCTGTGACATGAAAGG	
CD1D1		-1.46195839	-0.084498452	1.377459938		0.028787	0.886047215	0.02663035	ILMN_2734212	GAACTAGAAAGCATACTTCCTGCCCAAACAGACGCTCTGAGGTTAGTTG	Mus musculus CD1d1 antigen (Cd1d1), mRNA.
CDKN1A		-0.598236148	0.649996258	1.248232406		0.2810181	0.243870608	0.02766547	ILMN_2634083	CATCCTGGTCTGGACTGTCTACCCTTAGCCCGCACCCCAAGAACATGTA	Mus musculus cyclin-dependent kinase inhibitor 1A (P21) (Cdkn1a), mRNA.
CFD		-2.965653662	0.530765528	3.496419189		0.0049065	0.536798053	0.0010017	ILMN_2835423	CAGTCGAAGGTGTGGTTACGTGGGGCTCTCGCGTCTGTGGCAATGGCA	Mus musculus complement factor D (adipsin) (Cfd), mRNA.
CIDEA		-1.801244902	-0.559559857	1.241685045		0.0150816	0.385987296	0.05452063	ILMN_1215446	GACGGGACAGTTCCTGGTCTATGCGGGCACATACATGCTCCGAGTACT	Mus musculus cell death-inducing DNA fragmentation factor, alpha subunit-like effector A (Cidea), mRNA.
CIDEC		-1.456853318	-0.138919218	1.317934099		0.0081337	0.761195691	0.00924771	ILMN_1222679	GAGGTGTGCGAGAGAGTGTTAGAGGTGGAGATTAACTAAAGCCGGCAT	Mus musculus cell death-inducing DFFA-like effector c (Cidec), mRNA.
CLDN11		-1.645730543	-1.42116018	0.224570363		0.0191203	0.036851878	0.69063747	ILMN_1246139	GTGTCTAAGACTCTGGATACTGCAAGCTCCGTCCGGTGCATTTGTTCAG	Mus musculus claudin 11 (Cldn11), mRNA.
COX8B		-2.449745171	-0.250312233	2.199432937		0.0265011	0.796554407	0.03034856	ILMN_2727520	CGTTGGCTTCATGGTTCCAGCAGGATGGGTCTTAGCCCACTTGGAGAG	Mus musculus cytochrome c oxidase, subunit VIIIb (Cox8b), mRNA.
GNA14		0.487424158	-0.52936533	-1.016789488		0.3000355	0.262600443	0.03319393	ILMN_2597778	GCGCTGTGCCTTTCTGGATACTAAGAATACACTGTTCTACCCTGAACAC	Mus musculus guanine nucleotide binding protein, alpha 14 (Gna14), mRNA.
HAVCR1		-0.172270347	1.403494432	1.575764778		0.7857277	0.045698769	0.01981639	ILMN_2604307	AAGCTTTGCAGAACGCAGCGGTTGTGCATTCCCGAGCTGAAGACAACA	Mus musculus hepatitis A virus cellular receptor 1 (Havcr1), mRNA.
HP		-2.096151341	0.392517347	2.488668689		0.0132898	0.587818322	0.00317183	ILMN_2668509	CTGTTGTCACTCTCCTGCTCTGGGGTCAGCTTTTTGCTGTGGAGTTGGG	Mus musculus haptoglobin (Hp), mRNA.
HP		-2.204083306	0.44858963	2.652672936		0.0217303	0.593855579	0.00538841	ILMN_2668510	CTCTCCTGCTCTGGGGTCAGCTTTTTGCTGTGGAGTTGGGCAATGATGC	Mus musculus haptoglobin (Hp), mRNA.
HP		-2.332394507	0.611622015	2.944016523		0.0117124	0.44034818	0.00181362	ILMN_2944824	ACGAGTCCCGTTGGGGTCCAGCCTATCTTGAACGAGCACACCTTCTGT	Mus musculus haptoglobin (Hp), mRNA.
IGFBP5		-0.499217044	-1.072298018	-0.573080974		0.272493	0.031436343	0.18029713	ILMN_2964324	GGATAGTACAGTTCAGACAAGACTCCTTCAGATTCCGAGACGCCTACCG	Mus musculus insulin-like growth factor binding protein 5 (Igfbp5), mRNA.
IL4I1		-0.391947595	-1.081478706	-0.689531111		0.3802022	0.029367298	0.11131137	ILMN_2733778	CCCAGCTCCTAAGCCAGCCCTCTTCAGGGCAGACAGACCACCTACACT	Mus musculus interleukin 4 induced 1 (Il4i1), mRNA.
ITIH4		-0.746467905	0.417565978	1.164033883		0.1420903	0.394031883	0.02270197	ILMN_2718431	CACCTTATGCCAACAGGGACGCCTGTGAGGCCGAGACCTTGATGGGAA	Mus musculus inter alpha-trypsin inhibitor, heavy chain 4 (Itih4), mRNA.
KRT20		0.083357367	1.757084824	1.673727457		0.8930599	0.015346426	0.01327319	ILMN_2907285	GTGAACGGGTTCTCCAGGGAGGCAACTTCCCAGTTAATCTCATTGTCTC	Mus musculus keratin 20 (Krt20), mRNA.
LOC100043671		-1.456136503	-0.593052178	0.863084325		0.0369099	0.351242413	0.15502824	ILMN_1258600	TCTGTCCACTTGTTCACAAAGCAGCCTTCACACGTGTCAGTGAGAGTTC	PREDICTED: Mus musculus hypothetical protein LOC100043671 (LOC100043671), mRNA.
MFSD2		-1.051508402	0.381609069	1.433117471		0.097658	0.522914016	0.02253908	ILMN_1225764	AGGGCTGCTACTGTGAATATGCCAAGGACTGACTGGGCCTAGCTCGGA	Mus musculus major facilitator superfamily domain containing 2 (Mfsd2), mRNA.
MYCL1		-0.022587085	1.064445119	1.087032205		0.9557901	0.022773331	0.01412011	ILMN_1221750	GGGACTCCTGGAACTATCTTGGGAGGACAAGTGGTGAACAGGCTAAAG	Mus musculus v-myc myelocytomatosis viral oncogene homolog 1, lung carcinoma derived (avian) (Mycl1), mRNA.
MYL1		-1.077625097	-0.343423488	0.734201609		0.0333534	0.451390027	0.10004509	ILMN_2878542	GATAATCTCAAGTCCACACACCACCGTTATCATCTACTTGGGTCCACAA	Mus musculus myosin, light polypeptide 1 (Myl1), mRNA.
NNMT		-1.199571192	0.25428225	1.453853442		0.0678093	0.674137856	0.0229501	ILMN_2885277	CTCCCTAGTGGGGCGAAAGCCAGGCAGATCTGAATGACATCCTGTGAT	Mus musculus nicotinamide N-methyltransferase (Nnmt), mRNA.
ORM1		-2.030115548	-0.101961618	1.92815393		0.0352627	0.905436355	0.03164228	ILMN_1226935	CCTTTGCCCACCTTATAGTGCTGAGGAAACATGGGGCCTTCATGCTTGC	Mus musculus orosomucoid 1 (Orm1), mRNA.
S3-12		-1.472158014	0.190004481	1.662162495		0.0228048	0.736759772	0.00826673	ILMN_2588249	CCTTAGTGTCTGCTTCACTCAAGCTGGTAGAACAGGCTACTCGCTGCAC	Mus musculus plasma membrane associated protein, S3-12 (S3-12), mRNA.
SAA3		-0.78514295	0.678302447	1.463445398		0.1322338	0.187289026	0.00786362	ILMN_2772632	GAGGACTCAAGAGCTGACCAGTTTGCCAATGAGTGGGGCCGGAGTGGC	Mus musculus serum amyloid A 3 (Saa3), mRNA.
SCD1		-1.647443514	-0.537645069	1.109798445		0.0044752	0.263470449	0.02437171	ILMN_1237375	CCAGTCAAAGTGCAAGACTACCTACCCACTGCCATGAAAACCATTGCAG	Mus musculus stearoyl-Coenzyme A desaturase 1 (Scd1), mRNA.
SCIN		-0.002361753	-1.293221152	-1.290859399		0.9945273	0.003086022	0.00188657	ILMN_1259174	GCTTCTAAGCATTTCCCCGTCTGCTACTCTGTTTGCAGTGAGCTTTACTT	Mus musculus scinderin (Scin), mRNA.
SERPINA3C		-1.001675207	0.217593835	1.219269043		0.0171768	0.550762992	0.00373395	ILMN_2730054	CAAGGGACTCATCTCAGACCTGGATACGGATACACTGATGGTGCTGGT	Mus musculus serine (or cysteine) peptidase inhibitor, clade A, member 3C (Serpina3c), mRNA.
SERPINA3M		-0.885792445	0.417494031	1.303286476		0.03249	0.270410176	0.00270448	ILMN_2728473	CCTCTTTATGGCCAAAGTCACTAACCCCAAGTGAACCTAAAGCTCCCCA	Mus musculus serine (or cysteine) peptidase inhibitor, clade A, member 3M (Serpina3m), mRNA.
SERPINA3N		-1.378347276	0.440050877	1.818398152		0.0343426	0.453636705	0.00575328	ILMN_1246800	CCCCTGGCACTCCTACTTAGAACAAAGTAGCCTTTCTTTTAGTTCCCAGC	Mus musculus serine (or cysteine) peptidase inhibitor, clade A, member 3N (Serpina3n), mRNA.
SGK2		0.533528881	1.0746424	0.541113519		0.1507394	0.010434508	0.11899333	ILMN_2827080	GGCTGCCCAGAAACCGTCTGGTGGCTTCCTTTAGTGTGTCGTAAATCTC	Mus musculus serum/glucocorticoid regulated kinase 2 (Sgk2), mRNA.
SGK2		0.639027332	1.000316869	0.361289537		0.0772857	0.011458472	0.25746565	ILMN_2827081	GAGAGAAAGGGGAGGATGTAGGTGACCAGCACTCTGGGAGAGAGCCTC	Mus musculus serum/glucocorticoid regulated kinase 2 (Sgk2), mRNA.
SLC1A3		-1.259241472	0.321836021	1.581077493		0.040451	0.562001189	0.00954689	ILMN_2634317	CCCGGGCTCTGCCTATGTGTGTACCCACTGTGGACTGGGAAACTTCACT	Mus musculus solute carrier family 1 (glial high affinity glutamate transporter), member 3 (Slc1a3), mRNA.
SLC4A1		0.52824231	-0.744134243	-1.272376553		0.0751733	0.018739204	0.00039945	ILMN_1227675	CGCTCTTCCCCCACCGCCGTGCTTGGGAATAGGTTTTGCCAATAAACGT	Mus musculus solute carrier family 4 (anion exchanger), member 1 (Slc4a1), mRNA.
SLC5A3		0.750679233	1.037239005	0.286559772		0.0513856	0.012004863	0.38412317	ILMN_1233078	CCCAGTGGCTTCCATGGGTCATTCAGAGGCAGAAACACCAGTAGATGC	Mus musculus solute carrier family 5 (inositol transporters), member 3 (Slc5a3), mRNA.
TMEM174		0.249557844	-0.848911432	-1.098469276		0.414559	0.015675558	0.00224195	ILMN_1216425	GGCTGCCCCCAAGAGAGATACAGGAATTGTCAGGTCTTGAAGGTTTTG	Mus musculus transmembrane protein 174 (Tmem174), mRNA.
TRF		-1.477109112	0.245021332	1.722130444		0.0175221	0.648774584	0.00498246	ILMN_2485323	CTGGGGTAGACAGAACCGCTGGTTGGAACATCCCTATGGGCATGCTGT	Mus musculus transferrin (Trf), mRNA.

Database:molecular function Name:calcium ion binding ID:GO:0005509

C=479; O=5; E=0.94; R=5.32; rawP=0.0022; adjP=0.0336

Index	UserID	Value	Gene Symbol	Gene Name	EntrezGene	Ensembl
1	ILMN_2883392	NA	S100a11	S100 calcium binding protein A11 (calgizzarin)	20195	ENSMUSG0000027907
2	ILMN_2803674	NA	S100a9	S100 calcium binding protein A9 (calgranulin B)	20202	ENSMUSG0000056071
3	ILMN_2712120	NA	S100a6	S100 calcium binding protein A6 (calcyclin)	20200	ENSMUSG0000001025
4	ILMN_2691780	NA	Myl3	myosin, light polypeptide 3	17897	ENSMUSG0000059741
5	ILMN_2710905	NA	S100a8	S100 calcium binding protein A8 (calgranulin A)	20201	ENSMUSG0000056054

Database:cellular component Name:cytoplasmic membrane-bounded vesicle ID:GO:0016023

C=506; O=6; E=1.00; R=6.01; rawP=0.0004; adjP=0.0088

Index	UserID	Value	Gene Symbol	Gene Name	EntrezGene	Ensembl
1	ILMN_2712986	NA	Chi3l3	chitinase 3-like 3	12655	ENSMUSG0000040809
2	ILMN_1236889	NA	Selp	selectin, platelet	20344	ENSMUSG0000026580
3	ILMN_2669486	NA	Oxt	oxytocin	18429	ENSMUSG0000027301
4	ILMN_2714796	NA	Coro1a	coronin, actin binding protein 1A	12721	ENSMUSG0000030707
5	ILMN_1228475	NA	Ulk1	unc-51 like kinase 1	22241	ENSMUSG0000029512
6	ILMN_2766604	NA	Camp	cathelicidin antimicrobial peptide	12796	ENSMUSG0000038357

Liver

Database:molecular function Name:catalytic activity ID:GO:0003824
C=5105; O=27; E=11.04; R=2.45; rawP=5.83e-07; adjP=4.55e-05

Index	UserID	Value	Gene Symbol	Gene Name	EntrezGene	Ensembl
1	230073	NA	Ddx58	DEAD (Asp-Glu-Ala-Asp) box polypeptide 58	230073	ENSMUSG00000040296
2	107569	NA	Nt5c3	5'-nucleotidase, cytosolic III	107569	ENSMUSG00000029780
3	76654	NA	Upp2	uridine phosphorylase 2	76654	ENSMUSG00000026839
4	240549	NA	Gm4952	predicted gene 4952	240549	ENSMUSG00000071633
5	225913	NA	Dak	dihydroxyacetone kinase 2 homolog (yeast)	225913	ENSMUSG00000034371
6	58185	NA	Rsad2	radical S-adenosyl methionine domain containing 2	58185	ENSMUSG00000020641
7	13119	NA	Cyp4a14	cytochrome P450, family 4, subfamily a, polypeptide 14	13119	ENSMUSG00000028715
8	21743	NA	Inmt	indolethylamine N-methyltransferase	21743	ENSMUSG00000003477
9	17857	NA	Mx1	myxovirus (influenza virus) resistance 1	17857	NULL
10	17246	NA	Mdm2	transformed mouse 3T3 cell double minute 2	17246	ENSMUSG00000020184
11	14081	NA	Acsl1	acyl-CoA synthetase long-chain family member 1	14081	ENSMUSG00000018796
12	71911	NA	Bdh1	3-hydroxybutyrate dehydrogenase, type 1	71911	ENSMUSG00000046598
13	14857	NA	Gsta1	glutathione S-transferase, alpha 1 (Ya)	14857	ENSMUSG00000074183
14	67307	NA	Pbld2	phenazine biosynthesis-like protein domain containing 2	67307	ENSMUSG00000020068
15	64697	NA	Keg1	kidney expressed gene 1	64697	ENSMUSG00000024694
16	12304	NA	Pdia4	protein disulfide isomerase associated 4	12304	ENSMUSG00000025823
17	24110	NA	Usp18	ubiquitin specific peptidase 18	24110	ENSMUSG00000030107
18	21822	NA	Tgtp1	T cell specific GTPase 1	21822	ENSMUSG00000078922
19	20620	NA	Plk2	polo-like kinase 2	20620	ENSMUSG00000021701
20	15360	NA	Hmgcs2	3-hydroxy-3-methylglutaryl-Coenzyme A synthase 2	15360	ENSMUSG00000027875
21	14073	NA	Faah	fatty acid amide hydrolase	14073	ENSMUSG00000034171
22	15496	NA	Hsd3b5	hydroxy-delta-5-steroid dehydrogenase, 3 beta- and steroid delta-isomerase 5	15496	ENSMUSG00000038092
23	70789	NA	Kynu	kynureninase (L-kynurenine hydrolase)	70789	ENSMUSG00000026866
24	231655	NA	Oasl1	2'-5' oligoadenylate synthetase-like 1	231655	ENSMUSG00000041827
25	60525	NA	Acss2	acyl-CoA synthetase short-chain family member 2	60525	ENSMUSG00000027605
26	68636	NA	Fahd1	fumarylacetoacetate hydrolase domain containing 1	68636	ENSMUSG00000045316
27	74147	NA	Ehhadh	enoyl-Coenzyme A, hydratase/3-hydroxyacyl Coenzyme A dehydrogenase	74147	ENSMUSG00000022853

Database:biological process Name:defense response ID:GO:0006952
C=803; O=13; E=1.72; R=7.55; rawP=8.70e-09; adjP=2.38e-06

Index	UserID	Value	Gene Symbol	Gene Name	EntrezGene	Ensembl
1	21822	NA	Tgtp1	T cell specific GTPase 1	21822	ENSMUSG00000078922
2	230073	NA	Ddx58	DEAD (Asp-Glu-Ala-Asp) box polypeptide 58	230073	ENSMUSG00000040296
3	56312	NA	Nupr1	nuclear protein 1	56312	ENSMUSG00000030717
4	18489	NA	Reg3b	regenerating islet-derived 3 beta	18489	ENSMUSG00000071356
5	15958	NA	Ifit2	interferon-induced protein with tetratricopeptide repeats 2	15958	ENSMUSG00000045932
6	15959	NA	Ifit3	interferon-induced protein with tetratricopeptide repeats 3	15959	ENSMUSG00000074896
7	58185	NA	Rsad2	radical S-adenosyl methionine domain containing 2	58185	ENSMUSG00000020641
8	19695	NA	Reg3g	regenerating islet-derived 3 gamma	19695	ENSMUSG00000030017
9	70789	NA	Kynu	kynureninase (L-kynurenine hydrolase)	70789	ENSMUSG00000026866
10	66438	NA	Hamp2	hepcidin antimicrobial peptide 2	66438	ENSMUSG00000056978
11	17857	NA	Mx1	myxovirus (influenza virus) resistance 1	17857	NULL
12	100689	NA	Spon2	spondin 2, extracellular matrix protein	100689	ENSMUSG00000037379
13	231655	NA	Oasl1	2'-5' oligoadenylate synthetase-like 1	231655	ENSMUSG00000041827

Kidney

Database:cellular component Name:lipid particle ID:GO:0005811

C=43; O=4; E=0.11; R=37.95; rawP=3.58e-06; adjP=8.83e-05

Index	UserID	Value	Gene Symbol	Gene Name	EntrezGene	Ensembl
1	ILMN_2588249	NA	Plin4	perilipin 4	57435	ENSMUSG00000002831
2	ILMN_1215446	NA	Cidea	cell death-inducing DNA fragmentation factor, alpha subunit-like effector A	12683	ENSMUSG00000024526
3	ILMN_1222679	NA	Cidec	cell death-inducing DFFA-like effector c	14311	ENSMUSG00000030278
4	ILMN_1222246	NA	Plin2	perilipin 2	11520	ENSMUSG00000028494

Database:molecular function Name:carboxylic acid binding ID:GO:0031406

C=178; O=4; E=0.38; R=10.48; rawP=0.0005; adjP=0.0145

Index	UserID	Value	Gene Symbol	Gene Name	EntrezGene	Ensembl
1	ILMN_2599794	NA	Apoc1	apolipoprotein C-I	11812	ENSMUSG00000040564

2	ILMN_2634317	NA	Slc1a3	solute carrier family 1 (glial high affinity glutamate transporter), member 3	20512	ENSMUSG00000005360
3	ILMN_1258600	NA	Acaca	acetyl-Coenzyme A carboxylase alpha	107476	ENSMUSG00000020532
4	ILMN_2738082	NA	Adipoq	adiponectin, C1Q and collagen domain containing	11450	ENSMUSG00000022878